

Article

Increasing Hydrogen Density with the Cation-Anion Pair BH_4^- - NH_4^+ in Perovskite-Type $\text{NH}_4\text{Ca}(\text{BH}_4)_3$

Pascal Schouwink ¹, Fabrice Morelle ², Yolanda Sadikin ¹, Yaroslav Filinchuk ² and Radovan Černý ^{1,*}

¹ Department of Quantum Matter Physics, Laboratory of Crystallography, University of Geneva, Quai Ernest-Ansermet 24, CH-1211 Geneva, Switzerland; E-Mails: pascal.schouwink@unige.ch (P.S.); yolanda.sadikin@unige.ch (Y.S.)

² Institute of Condensed Matter and Nanosciences, Université Catholique de Louvain, Place L. Pasteur 1, 1348 Louvain-la-Neuve, Belgium; E-Mails: fabrice.morelle@uclouvain.be (F.M.); yaroslav.filinchuk@uclouvain.be (Y.F.)

* Author to whom correspondence should be addressed; E-Mail: radovan.cerny@unige.ch; Tel.: +41-22-379-6450; Fax: +41-22-379-6108.

Academic Editor: Craig M. Jensen

Received: 3 March 2015 / Accepted: 22 July 2015 / Published: 6 August 2015

Abstract: A novel metal borohydride ammonia-borane complex $\text{Ca}(\text{BH}_4)_2 \cdot \text{NH}_3\text{BH}_3$ is characterized as the decomposition product of the recently reported perovskite-type metal borohydride $\text{NH}_4\text{Ca}(\text{BH}_4)_3$, suggesting that ammonium-based metal borohydrides release hydrogen gas via ammonia-borane-complexes. For the first time the concept of proton-hydride interactions to promote hydrogen release is applied to a cation-anion pair in a complex metal hydride. $\text{NH}_4\text{Ca}(\text{BH}_4)_3$ is prepared mechanochemically from $\text{Ca}(\text{BH}_4)_2$ and NH_4Cl as well as NH_4BH_4 following two different protocols, where the synthesis procedures are modified in the latter to solvent-based ball-milling using diethyl ether to maximize the phase yield in chlorine-free samples. During decomposition of $\text{NH}_4\text{Ca}(\text{BH}_4)_3$ pure H_2 is released, prior to the decomposition of the complex to its constituents. As opposed to a previously reported adduct between $\text{Ca}(\text{BH}_4)_2$ and NH_3BH_3 , the present complex is described as NH_3BH_3 -stuffed α - $\text{Ca}(\text{BH}_4)_2$.

Keywords: metal borohydride; perovskite; ammonium; ammonia-borane; protic-hydridic; hydrogen storage

1. Introduction

Complex hydrides material design has undergone major progress since the first reports suggesting LiBH_4 as a solid state hydrogen storage material [1]. Semi-empirical chemical concepts combining the stabilities of the less stable and more stable borohydrides [2], for instance, have given way to more profound concepts that exploit different kinds of weak interaction [3]. Recently, we reported on a large family of mixed-metal borohydrides crystallizing in the perovskite structure type, the latter being a prime example of functional materials design [4]. As a very stable structure type, the perovskite form allows one to study the behavior of a large range of different metals in a borohydride environment, but also to apply an immense toolbox developed throughout decades of metal-oxide perovskite design. The most simple concept comprises cation-substitution on the cuboctahedral *A*- and octahedral *B*-sites of a material generalized as $AB(\text{BH}_4)_3$. A logical further step is to explore anion-mixing on the ligand site. It was shown that the borohydride perovskite host readily takes up halide anions on the borohydride site [4]. In this context, it comes to mind to test the nitrogen-based hydrogen molecules, which are currently being vigorously investigated as means to tailor hydrogen release temperatures [3]. Recently we described interesting lattice instabilities in the metal borohydride perovskites where supposedly close homopolar dihydrogen contacts between adjacent borohydride anions stabilize lattice distortions in the high-temperature phase of $AB(\text{BH}_4)_3$, while these are most commonly destabilized by temperature in metal oxide or halide perovskites [4].

Aside from ammonium borohydride NH_4BH_4 itself [5–7], the ammonium cation has been rather neglected by the hydrogen storage community, and so far considered only in conjunction with higher boranes such as $\text{NH}_4\text{B}_3\text{H}_8$ [8], $(\text{NH}_4)_2\text{B}_{10}\text{H}_{10}$ or $(\text{NH}_4)_2\text{B}_{12}\text{H}_{12}$ [9] which impede the borazine evolution during thermolysis thanks to their stable borane cages, but never as a building block in a metal-based material. Attempts to tailor the thermal stability of NH_4BH_4 , which decomposes slowly at room temperature (RT), have also been carried out to develop it as solid state hydrogen storage material [7,10].

The underlying concept of incorporating NH_4^+ was to increase the gravimetric hydrogen capacity ρ_m of perovskite-type $\text{KCa}(\text{BH}_4)_3$ by monovalent cation substitution on the K-site or divalent cation substitution on the Ca-site. Attempts to achieve this by the substitution K^+-Na^+ or $\text{Ca}^{2+}-\text{Mg}^{2+}$ fail, as the hypothetical compounds $\text{NaCa}(\text{BH}_4)_3$, $\text{KMg}(\text{BH}_4)_3$ or $\text{NaMg}(\text{BH}_4)_3$ all come to lie outside the experimentally established stability field of the structure type within borohydrides [4]. The ionic radius of monovalent NH_4^+ (1.43 Å), on the other hand, is close to that of K^+ (1.33 Å) and ammonium easily substitutes for potassium in many metal halides. The calculated tolerance and octahedral factors suggest $\text{NH}_4\text{Ca}(\text{BH}_4)_3$ to be a stable compound. Its thermal stability and structure were recently reported in [4], accomplishing the long-term RT-stabilization of ammonium borohydride NH_4BH_4 , with the extreme hydrogen density of 24.5 wt % H_2 in a metal ammonium borohydride, $\text{NH}_4\text{Ca}(\text{BH}_4)_3$, with a high density of $\rho_m = 15.7$ wt % H_2 . Herein, we modify the reported synthesis based on ammonium chloride NH_4Cl to produce chlorine-free samples, taking up this study and focus on the actual decomposition mechanism of $\text{NH}_4\text{Ca}(\text{BH}_4)_3$ via an unknown ammonia-borane complex, which is obtained as a single phase sample thanks to the modified procedure and whose structure is solved on the basis of synchrotron X-ray powder diffraction. The vividly applied concept to tailor hydrogen release properties, the hetero-polar contact between protic and hydridic hydrogen, is thus extended for the first time to a cation-anion pair, $\text{NH}_4^+-\text{BH}_4^-$, in a metal borohydride. The presented concept of

cation-substitution by ammonium is easily extended to a large number of previously reported mixed-metal borohydrides [11].

2. Results and Discussion

The substitution of K^+ for NH_4^+ results in a stable compound $NH_4Ca(BH_4)_3$, which is presently investigated by means of two different synthetic mechanochemistry routes using different sources of the ammonium molecule. While the first employs a metathesis reaction based on ammonium chloride, in the second, chlorine-free, approach, NH_4BH_4 is loaded at low temperatures in the milling jar and reacted directly with $Ca(BH_4)_2$ in an addition reaction. The Cl-approach results in better crystallized compounds and a less complex phase composition (of novel phases) in as-milled samples, which is why the decomposition is discussed for these samples, despite the chlorine-content. On the other hand, the main decomposition product occurring during thermolysis of both samples is obtained as a well crystallized single phase composition in the NH_4BH_4 -based one, when milled in the presence of a solvent (ether). The crystal structure of the main decomposition product is hence solved and discussed on the basis of these data.

2.1. Formation of $NH_4Ca(BH_4)_3$

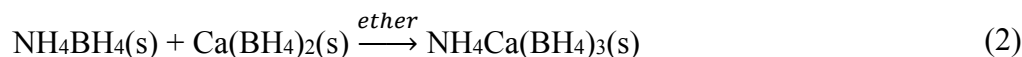
In samples synthesized from NH_4Cl , perovskite-type $NH_4Ca(BH_4)_3$ is formed according to a general metathesis reaction used for borohydride-perovskites, developed for cases when one of the precursors cannot be provided as a borohydride:



A number of different nominal $NH_4Cl:Ca(BH_4)_2:LiBH_4$ compositions were investigated, $NH_4Ca(BH_4)_3$ forming in the less NH_4Cl -rich mixtures 1:1:1, 1:2:1 and 1:2:2, but neither in 2:2:1 nor 3:1:3. At least three other phases with very low decomposition temperatures were observed as impurities or the main phase in 2:2:1 and 3:1:3 mixtures in as-milled samples prepared from the chloride, presumably containing NH_4^+ as indicated by their low decomposition temperatures, but these could not be identified and will not be further discussed presently.

The formation of $NH_4Ca(BH_4)_3$ from the borohydrides, *i.e.*, $Ca(BH_4)_2$ and NH_4BH_4 , was attempted in various trials. To this end milling jars were preliminarily cooled to 243 K, in order to stabilize NH_4BH_4 (unstable at RT) in a ratio 1:1 next to solid $Ca(BH_4)_2$. Soft milling (30 min at 500 rpm) of this mixture resulted in a multiphase powder with an unsatisfactory phase yield of $NH_4Ca(BH_4)_3$ (black curve in Figure 1). The low yield may be owed to partial decomposition of NH_4BH_4 , since the jars were not cooled during milling and the inside-temperature reached approximately 310 K.

The procedure was subsequently modified to a solvent-assisted protocol where diethyl ether was added to the mixture and the inside-temperature was kept below 270 K, resulting in a significantly improved phase yield of $NH_4Ca(BH_4)_3$ (blue curve in Figure 1). At temperature below RT, and neglecting impurities, the formation from the borohydrides can hence ideally be approximated as:



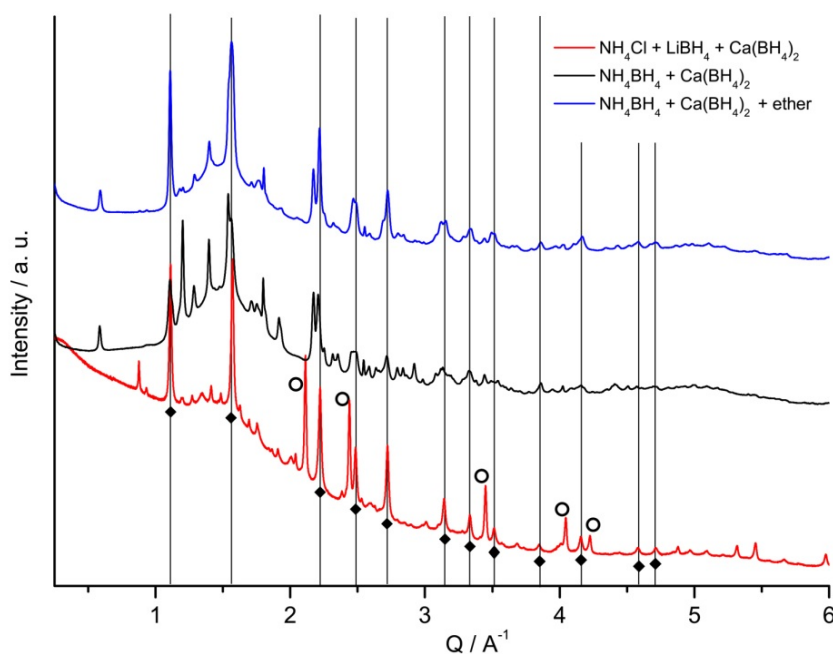


Figure 1. Room temperature synchrotron X-ray powder diffraction patterns shown for chloride-based (bottom curve, mixture 1:1:1), dry NH_4BH_4 -ballmilled (middle) and ether- NH_4BH_4 -ballmilled samples (top). Squares and vertical lines mark peak position of $\text{NH}_4\text{Ca}(\text{BH}_4)_3$, open circles correspond to LiCl .

Despite differences in the phase composition with respect to impurities the perovskite-type borohydride $\text{NH}_4\text{Ca}(\text{BH}_4)_3$ is the main phase in both the presently discussed chloride (1:1:1) and ether-based approaches. Furthermore, the fact that the lattice parameter a is identical within error (5.655(3) and 5.651(5) Å at 313 K for $\text{NH}_4\text{Ca}(\text{BH}_4)_3$ produced by chloride- and ether-based ball milling) as indicated by identical Bragg peak position in Figure 1 demonstrates the efficiency of Reaction (1) in terms of its capability to produce a borohydride-pure product without chloride on the anion-site, showing that the metathesis is completed in such an approach.

2.2. Thermolysis of $\text{NH}_4\text{Ca}(\text{BH}_4)_3$

The ammonium metal-borohydride perovskite $\text{NH}_4\text{Ca}(\text{BH}_4)_3$ starts decomposing at approximately 380 K in both, chloride and chloride-free samples. The respective temperature-dependent *in-situ* synchrotron diffraction data are shown for the chloride sample in Figure 2. The suggested decomposition mechanism for the chloride synthesis involves the formation of $\beta\text{-Ca}(\text{BH}_4)_2$ and LiBH_4 via an intermediate decomposition product, which occurs as an impurity already in some as milled mixtures in both approaches (Supplementary Figures S1 and S2). This decomposition intermediate is an unreported AB-complex of $\text{Ca}(\text{BH}_4)_2$ ($\text{AB} = \text{NH}_3\text{BH}_3$) and is discussed in detail below.

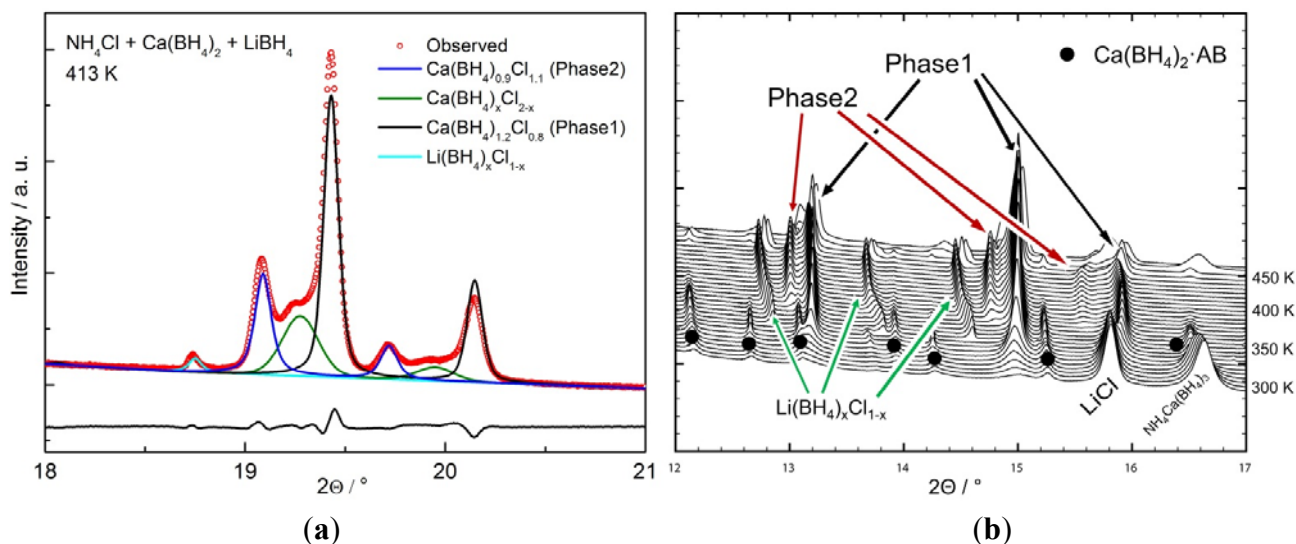


Figure 2. (a) Selected part of Rietveld plot at 413 K for the chloride-based mixture 1:1:1. Three different compositions of $\text{Ca}(\text{BH}_4)_x\text{Cl}_{2-x}$ were modeled in addition to $\text{Li}(\text{BH}_4)_x\text{Cl}_{1-x}$. The difference curve to the fit is shown on the bottom; (b) Close-up on *in-situ* diffraction data showing crystallization and chlorine uptake by $\text{Ca}(\text{BH}_4)_x\text{Cl}_{2-x}$. The models of $\text{Ca}(\text{BH}_4)_{0.9}\text{Cl}_{1.1}$ and $\text{Ca}(\text{BH}_4)_{1.2}\text{Cl}_{0.8}$ at 413 K (left) correspond to Phase 1 and Phase 2 in the temperature ramp.

As temperature is increased, calcium borohydride then proceeds to take up chlorine according to $\text{Ca}(\text{BH}_4)_{2-x}\text{Cl}_x$ in Cl-mixtures, as discussed below. Interestingly, chloride seems to stabilize the β -phase of $\text{Ca}(\text{BH}_4)_2$, which has previously been observed [12], whereas in ether-milled samples the phase composition *post-decomposition* is a mixture of β - and γ -phases. Ideally, the decomposition mechanism for the chloride-free protocol consists in inverting Reaction (2), *i.e.*, the stored NH_4BH_4 would be released. In reality, however, the decomposition involves the intermediate 1, *i.e.*, the novel AB-complex $\text{Ca}(\text{BH}_4)_2 \cdot \text{AB}$. Hence, while $\text{NH}_4\text{Ca}(\text{BH}_4)_3$ may be considered a means of storing (irreversibly) ammonium borohydride in the solid state, it cannot be released. The idealized decomposition mechanism of $\text{NH}_4\text{Ca}(\text{BH}_4)_3$ can therefore be written as:



While this reaction is stoichiometric and observed in the chloride free samples, the situation is more complex when the presence of chlorine is taken into account, leading to multiple processes releasing and absorbing chlorine which are outlined below.

Figure 3 shows the previously published [4] analysis of volatile decomposition products with the corresponding thermal and gravimetric signals, measured on the chloride-sample. Notably, there is no diborane released during the whole thermal decomposition of $\text{NH}_4\text{Ca}(\text{BH}_4)_3$, which in turn does release one molecule of hydrogen around 380 K (observed on Cl sample) and transforms to $\text{Ca}(\text{BH}_4)_2 \cdot \text{AB}$, in both chloride and ether milled samples, according to Reaction (3).

In chloride-based samples the decomposition proceeds directly to the AB-complex. This gas release is readily identified as the first mass loss in Figure 3, where mass spectrometry (top panel) shows that the released product's composition is nearly pure hydrogen (very small signal of NH_3 at 380 K). $\text{Ca}(\text{BH}_4)_2 \cdot \text{AB}$ then decomposes to release additional hydrogen above 400 K, accompanied by a minor

amount of ammonia NH_3 (Figure 3), similar to previously reported reaction mechanisms for AB complexes involving recovery of $\beta\text{-Ca}(\text{BH}_4)_2$ [13,14]. This corresponds to the second mass loss and is visible as a continuous evolution in the spectrometric detection of H_2 . The decomposition temperature of the AB complex compares quite well with those of the first two reported members of the metal borohydride AB family [15].

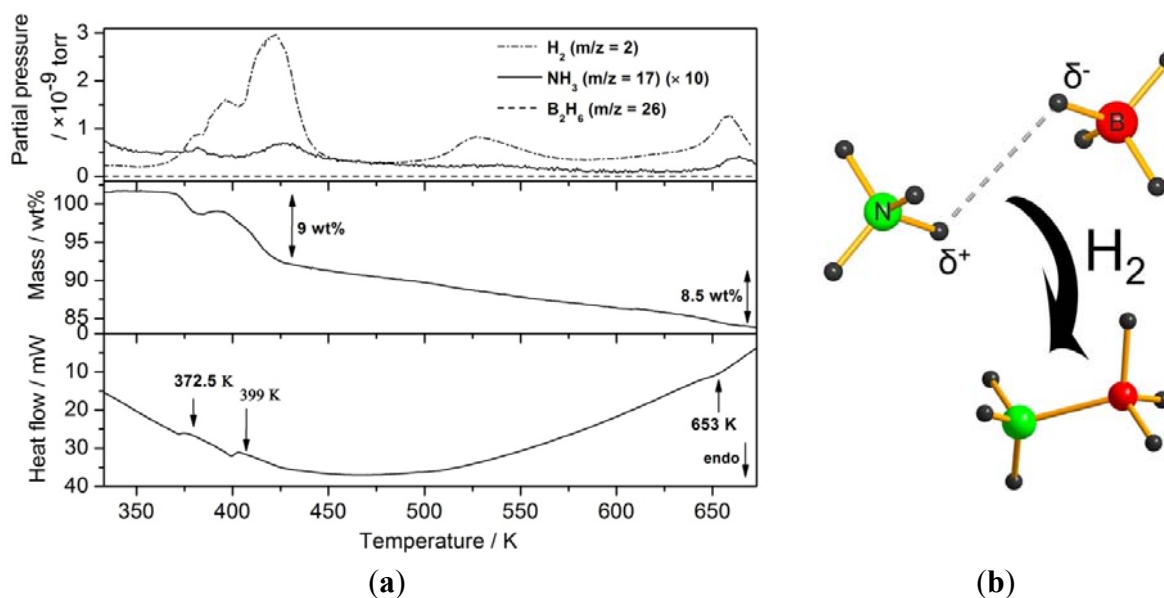
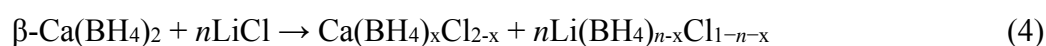


Figure 3. Simultaneous gas release and thermal analysis of the decomposition of $\text{NH}_4\text{Ca}(\text{BH}_4)_3$ under nitrogen flow (heating rate 5 K/min, chloride sample, reproduced from [4]). (a) Results from mass-spectrometry (MS), thermal gravimetric analysis (TGA) and differential scanning calorimetry (DSC), the signal corresponding to NH_3 has been multiplied $\times 10$; (b) Close heteronuclear dihydrogen contact between protic hydrogen pertaining to the ammonium cation and hydridic hydrogen from the borohydride anion facilitates hydrogen releases via AB.

2.2.1. Chloride Substitution in $\beta\text{-Ca}(\text{BH}_4)_2$

In the following we briefly discuss the release and uptake of chlorine by different phases during thermal decomposition of the mixture $\text{NH}_4\text{Cl}:\text{Ca}(\text{BH}_4)_2:\text{LiBH}_4$ 1:1:1 and referring to the *in-situ* diffraction data shown in Figure 2. Chloride substitution has recently been investigated by ball-milling $\text{CaCl}_2 + \text{Ca}(\text{BH}_4)_2$ [16]. Therein, anion-substitution is achieved by heating as-milled mixtures of unreacted precursors, which results in halide-substituted $\beta\text{-Ca}(\text{BH}_4)_{2-x}\text{Cl}_x$. The authors report different compositions with discrete lattice parameters depending on the nominal composition of precursors in the respective sample. The chlorine uptake by $\beta\text{-Ca}(\text{BH}_4)_2$ during the decomposition of $\text{NH}_4\text{Ca}(\text{BH}_4)_3$ is fundamentally different, since it is not CaCl_2 acting as a chlorine-source. In this case, the chlorine is provided by LiCl , which is formed during the metathesis Reaction (1). Concurring with the decomposition of the ammonium perovskite LiCl continuously transforms into hexagonal HT-phase $\text{Li}(\text{BH}_4)_x\text{Cl}_{1-x}$, which crystallizes together with halide-substituted $\beta\text{-Ca}(\text{BH}_4)_2$ (Figure 2) according to Reaction (4):



While the dissolution of chloride is known to stabilize the hexagonal HT-phase of LiBH_4 , we observe a hitherto unreported behavior of the HT-phase (β) of $\text{Ca}(\text{BH}_4)_2$. A detailed examination of the *in-situ* diffraction data provided in Figure 2 is essential to the following discussion. At approximately 350 K the remnant $\text{Ca}(\text{BH}_4)_2$ not reacted but amorphized during ball-milling starts recrystallizing, accompanying the formation and crystallization of the AB-complex $\text{Ca}(\text{BH}_4)_2 \cdot \text{AB}$. Despite the temperature increase the lattice parameters of $\beta\text{-Ca}(\text{BH}_4)_2$ decrease as crystallinity increases (see Bragg signal at 15° shifting to higher angles with temperature, in Figure 2), due to chlorine-uptake originating from LiCl , while the Li is used to form $\text{Li}(\text{BH}_4)_x\text{Cl}_{1-x}$. At temperatures of approximately 400 K, coinciding with the decomposition of the AB-complex in the chloride-based sample, halide-substituted $\beta\text{-Ca}(\text{BH}_4)_2$ abruptly forms two phases of well-defined chemical composition and discrete lattice parameters (labeled Phase1 and Phase2 in Figure 2), accompanied by a third phase of intermediate composition and much broader diffraction peaks. Rietveld refinement was performed on data collected at 413 K and including 3 different $\beta\text{-Ca}(\text{BH}_4)_x\text{Cl}_{2-x}$ compositions. The result of the refinement is shown in Figure 2. Two compositions $\text{Ca}(\text{BH}_4)_{0.9}\text{Cl}_{1.1}$ and $\text{Ca}(\text{BH}_4)_{1.2}\text{Cl}_{0.8}$ could be refined reliably corresponding to unit cell volumes of $194.8(9)$ and $185.3(7) \text{ \AA}^3$, respectively. The evolution of the cell volumes at higher temperature is shown in Supplementary Figure S3. These values are far below that of the reported unit cell volume of pure homoleptic $\beta\text{-Ca}(\text{BH}_4)_2$ at 305 K, 208.1 \AA^3 [17], in agreement with the smaller anion radius of Cl^- . The anion-composition of the third component corresponding to the broad signals in Figure 2 could not be determined reproducibly but is thought to lie between the two determined stoichiometries. The line width is approximately a factor 2.5 larger than in both other compositions. This may be due to a continuous distribution of chlorine dissolution on the BH_4 -site. But also a shorter coherence length could be at the origin of the signal-width, suggesting intermediate chemical compositions on very short length scales, for instance at the grain-boundaries between compositions $\text{Ca}(\text{BH}_4)_{0.9}\text{Cl}_{1.1}$ and $\text{Ca}(\text{BH}_4)_{1.2}\text{Cl}_{0.8}$. To our knowledge the coexistence of various discrete anion-compositions has not been reported for $\beta\text{-Ca}(\text{BH}_4)_2$, despite anion-substitution having been quite well studied in this compound [12,16].

2.2.2. Ether-Samples

In the samples which were prepared by ball milling solidified NH_4BH_4 in ether at low temperatures the decomposition mechanism is not influenced by the kinetics of chlorine-exchange between the involved pseudobinary compounds $\beta\text{-Ca}(\text{BH}_4)_2$ and LiBH_4 .

While the transformation of $\text{NH}_4\text{Ca}(\text{BH}_4)_3$ to the novel AB-complex is observed as in the chloride-sample, the decomposition now involves a further intermediate **2** (Supplementary Figure S2) that has not been characterized (T-interval 370–385 K, given the vicinity to the solved structure of $\text{Ca}(\text{BH}_4)_2 \cdot \text{AB}$ we assume **2** to be a further AB-complex, possibly a phase transformation then takes place at 380 K), but indexed to an orthorhombic cell of $a = 11.602$, $b = 14.339$, $c = 14.296 \text{ \AA}$, $V = 2378 \text{ \AA}^3$. This phase does not occur in chloride-syntheses. It is unlikely that there is a hydrogen loss occurring between intermediate **2** and $\text{Ca}(\text{BH}_4)_2 \cdot \text{AB}$, since the reported product of the first two decomposition steps of NH_4BH_4 is the diammoniate of diborane $[(\text{NH}_3)_2\text{BH}_2](\text{BH}_4)$, which itself is an isomer in equilibrium with AB [18], and no intermediate deprotonated molecule exists. Given the small stability field of approximately 5 K and the vicinity to the stability field of $\text{Ca}(\text{BH}_4)_2 \cdot \text{AB}$,

intermediate 2 may be a further AB-derivative of different stoichiometry, or merely a superstructure to $\text{Ca}(\text{BH}_4)_2 \cdot \text{AB}$, related by a polymorphic transformation.

In ether milled mixtures $\text{Ca}(\text{BH}_4)_2 \cdot \text{AB}$ begins to decompose to β - and γ - $\text{Ca}(\text{BH}_4)_2$ at 400 K, proceeding until 430 K (Supplementary Figure S2), which is in surprising agreement with the decomposition-onset of the previously reported AB-complex of $\text{Ca}(\text{BH}_4)_2$, determined at 398 K, and ending at 428 K [14]. Hence, while the second decomposition step follows the established mechanism of AB-complexes, the perovskite adds an additional hydrogen release prior to this.

We have not identified further decomposition products. The previously reported AB-complexed $\text{Ca}(\text{BH}_4)_2$ decomposes to its constituents. AB melts at 377 K therefore its possible existence cannot be determined from the diffraction patterns. A difference in structure between the two (discussed below) could suggest a slightly modified decomposition pathway, the reported AB-complex [14] possibly showing a greater predisposition to dissociate to $\text{Ca}(\text{BH}_4)_2$ and AB due to its structural topology, which is built of defined layers of both precursors, while $\text{Ca}(\text{BH}_4)_2 \cdot \text{AB}$ reported herein contains AB molecules whose nearest neighbor interactions are considered to be weaker with respect to those taking place in AB itself.

2.3. Crystal Structure of $\text{NH}_4\text{Ca}(\text{BH}_4)_3$

In the ammonium calcium borohydride perovskite the NH_4^+ cation occupies the A-site of the perovskite structure, where Ca is the B-cation and the BH_4^- anion is the ligand. We have chosen to model the structure in an ordered manner in a subgroup symmetry which allows for an identical unit cell metric to the primitive perovskite unit. A fully disordered structure can be modelled in $Pm-3m$, however the fit is not better. The ordered description is supported, albeit not fully justified, by X-ray diffraction data collected down to temperatures of 100 K which did not show a change in diffraction pattern that would suggest a phase transition due to ordering. All reported phase transitions in borohydride perovskites occur above RT without any further events down to 100 K [4,19].

Furthermore, the dominant weak interaction in $\text{NH}_4\text{Ca}(\text{BH}_4)_3$ is of attractive nature and structurally points towards an ordered model. Future neutron studies, as planned also for other metal borohydride perovskites may however result in a correction of this space group symmetry. Our structural description currently is in $P-43m$, which is a subgroup to $Pm-3m$, and allows maximizing homopolar dihydrogen contacts $\text{BH} \cdots \text{HB}$ between hydride anions, which are constrained to lower values by symmetry in other subgroups to $Pm-3m$, as for instance $P432$. One boron position and one nitrogen position provide orientation between the molecular species that are rotated by 90° around the principal cubic direction with respect to each other (Figure 4).

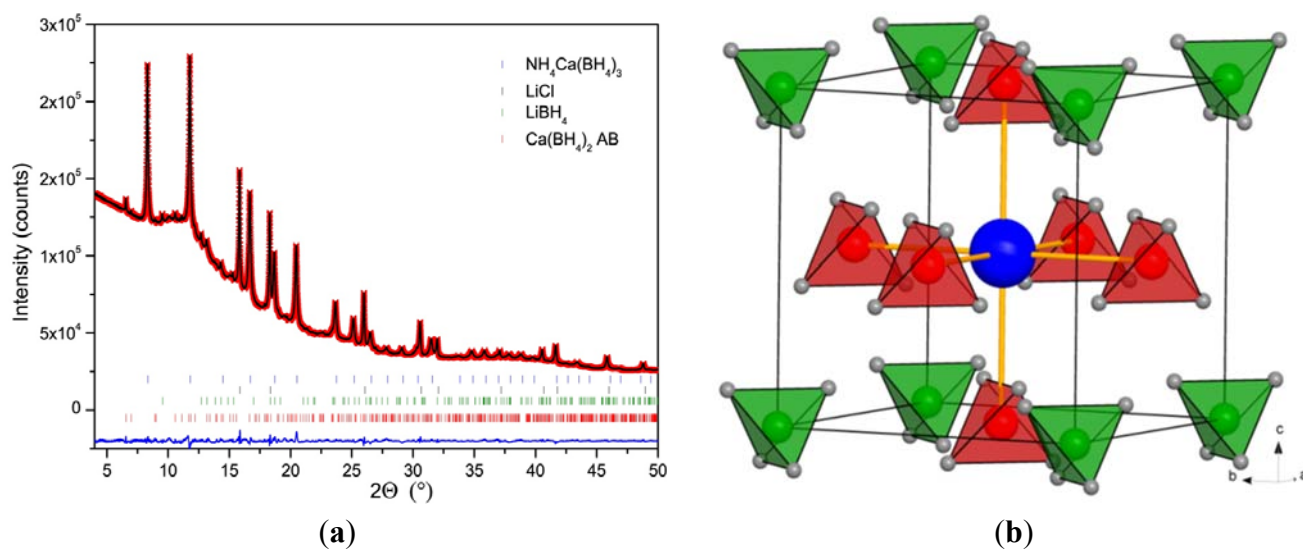


Figure 4. (a) Rietveld plot for the chloride-based synthesis of $\text{NH}_4\text{Ca}(\text{BH}_4)_3$, refined at 298 K; and (b) structural model in space group $P-43m$. NH_4^+ green, BH_4^- red, Ca blue.

2.4. Crystal Structure of $\text{Ca}(\text{BH}_4)_2 \cdot \text{NH}_3\text{BH}_3$

The dehydrogenation product of the ammonium borohydride perovskite is the calcium borohydride ammonia-borane complex $\text{Ca}(\text{BH}_4)_2 \cdot \text{AB}$, which contains one AB molecule per $\text{Ca}(\text{BH}_4)_2$ unit and whose structure was solved *ab-initio* on a single phase sample from diffraction data collected at 414 K (Figure 5) during the decomposition of ether-milled $\text{NH}_4\text{Ca}(\text{BH}_4)_3$.

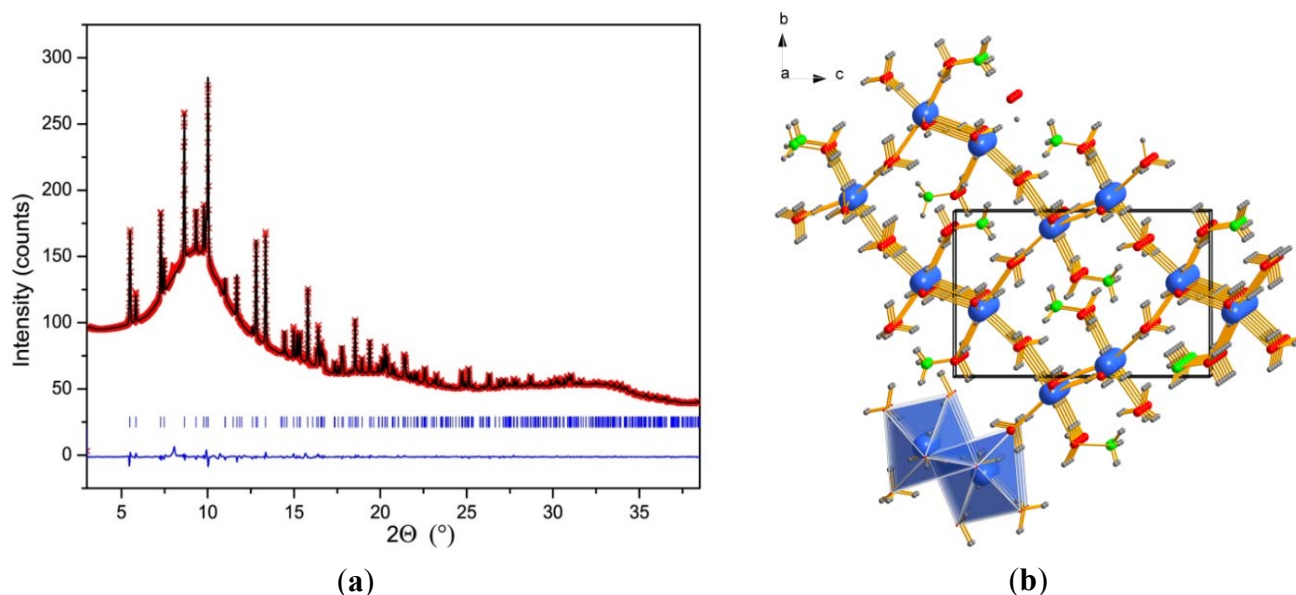


Figure 5. (a) Rietveld plot for the ether-milled sample, refined at 414 K, showing a pure phase composition of $\text{Ca}(\text{BH}_4)_2 \cdot \text{AB}$; (b) Corresponding structural model. N green, B red, H grey, Ca blue.

Interestingly, an AB complex of $\text{Ca}(\text{BH}_4)_2$ has previously been reported, which contains two AB molecules per unit cell [14] and was observed not during thermal composition, but obtained as an

adduct by ball-milling NH_3BH_3 with $\text{Ca}(\text{BH}_4)_2$. The structure therein was described as containing layers of AB alternating with layers (square lattice) of borohydride stacked along the long axis, b .

A close inspection of the structural model of $\text{Ca}(\text{BH}_4)_2 \cdot \text{AB}$ (Figure 6) reveals that the borohydride layers formed by a square lattice are conserved, however buckled by 90° . A further relationship is found in α - $\text{Ca}(\text{BH}_4)_2$ -like ribbons, running parallel to the a -axis in $\text{Ca}(\text{BH}_4)_2 \cdot \text{AB}$. These $\text{Ca}(\text{BH}_4)_2$ -ribbons are highlighted in the grey box in Figure 6. In this description the NH_3BH_3 molecules form a further one-dimensional structural element (zig-zag chain), which alternates with $\text{Ca}(\text{BH}_4)_2$ ribbons. In this context, the relationship between the AB-complex $\text{Ca}(\text{BH}_4)_2 \cdot \text{AB}$ and the reported $\text{Ca}(\text{BH}_4)_2 \cdot 2\text{AB}$ may therefore be described best as a reduction in dimensionality of the structural elements of the precursors in the former.

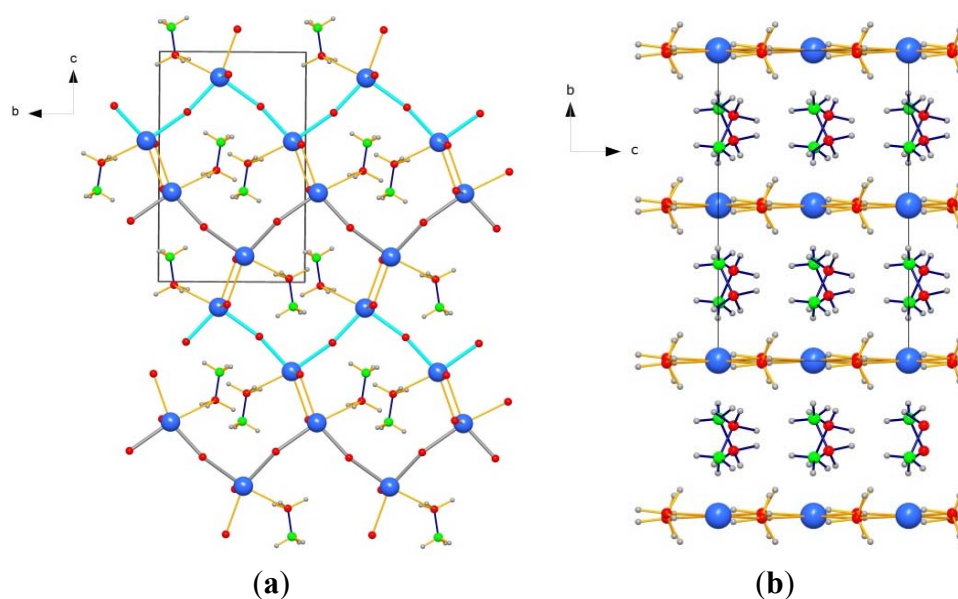


Figure 6. (a) Comparison of the crystal structure of $\text{Ca}(\text{BH}_4)_2 \cdot \text{AB}$; and (b) the reported $\text{Ca}(\text{BH}_4)_2 \cdot 2\text{AB}$ -complex [14]. On the left, the buckled square lattice of $\text{Ca}(\text{BH}_4)_2$ layers is drawn in light-blue and grey. N green, B red, H grey, Ca blue. H atoms have been omitted on BH_4 groups for sake of clarity on the left.

In α - $\text{Ca}(\text{BH}_4)_2$ the square lattice (layers) of $\text{Ca}-\text{BH}_4$ conserved in both AB-complexes is oriented perpendicular to the b -axis, while the ribbons conserved only in $\text{Ca}(\text{BH}_4)_2 \cdot \text{AB}$ connect these layers and run along the a -axis. If the buckled $\text{Ca}-\text{BH}_4$ square lattice (blue and grey sheets in Figure 6) is flattened out the α - $\text{Ca}(\text{BH}_4)_2$ structure is recovered in $\text{Ca}(\text{BH}_4)_2 \cdot \text{AB}$, however with 50% of the ribbons replaced by zig-zag chains of NH_3BH_3 . There is therefore no major reconstruction of the α - $\text{Ca}(\text{BH}_4)_2$ structure in this AB-complex.

The B-N lengths in $\text{Ca}(\text{BH}_4)_2 \cdot \text{AB}$ at 414 K amount to $1.613(5)$ Å, significantly longer than those in the reported $\text{Ca}(\text{BH}_4)_2 \cdot 2\text{AB}$ (1.546 Å at 298 K) and very close to those in solid NH_3BH_3 (1.592 Å) [13,14]. The intermolecular distances between hydride and proton ions $\text{BH} \cdots \text{HN}$ pertaining to adjacent AB molecules amount to 2.05 Å, as opposed to 1.736 Å in the reported $\text{Ca}(\text{BH}_4)_2 \cdot 2\text{AB}$, and are slightly larger to those in AB (2.02 Å). This attests to a larger degree of interaction to BH_4 groups as opposed to $\text{Ca}(\text{BH}_4)_2 \cdot 2\text{AB}$, which could lead to a slightly modified decomposition mechanism. The

closest refined BH \cdots HN distance between NH₃BH₃ and adjacent hydridic H⁻ of BH₄ groups is 2.02 Å, which is in quite good agreement with the values of 1.986 and 2.037 Å reported for Ca(BH₄)₂·2AB. The main difference hence lies in intermolecular AB contacts, which are significantly larger in Ca(BH₄)₂·AB. Nevertheless, we need to recall that the determination of interatomic hydrogen distances from X-ray powder diffraction data are severely biased by the application of restraints during refinement, and the determined values need not be very accurate.

3. Experimental Section

3.1. Synthesis

Ca(BH₄)₂, LiBH₄ and NH₄Cl were used as purchased from Sigma-Aldrich (Buchs, Switzerland). Chloride based samples were prepared by high-energy ball milling (mechanochemistry) in a Pulverisette P7 planetary ball mill (Fritsch, Idar-Oberstein, Germany). The ball-to-powder mass ratio was approximately 50, 60 milling cycles at 600 rpm of 2 min each were interrupted by 5 min cooling breaks to prevent heating and powder agglomeration on the walls of the milling jar. For the second approach based on NH₄BH₄, the latter was prepared according to ref. [20] with some minor modifications. Milling was performed in the Fritsch Pulverisette P7 planetary ball mill in a stainless steel vial cooled down to approximately 240 K prior to milling. The milling speed was set to 500 rpm and the ball to powder mass ratio was approximately 50 for both dry and liquid assisted (500 μL (350 mg) of Et₂O at 500 mg of sample mass) milling. The temperature of the milling jar was not kept low during milling. In the case of dry milling, the milling time was 30 min and the temperature of the jar was around 35 °C (308 K) at the end of the milling. In the case of the ether assisted milling, the milling time was of 5 min, resulting in a much smaller temperature increase during milling. The ether was removed by evacuating the sample directly after the milling.

3.2. Synchrotron Radiation X-ray Powder Diffraction (SR-XPD)

Synchrotron radiation powder X-ray diffraction (SR-PXD) data were collected at the Swiss Norwegian Beamlines of the European Synchrotron Radiation Facility (ESRF, Grenoble, France) and at the Materials Science Beamline of the Swiss Light Source (Paul Scherrer Institute, Villigen, Switzerland) 0.6888 and 0.8271 Å, respectively, as calibrated by a Si standard. Samples were loaded into 0.5 mm borosilicate capillaries. Structures were solved in direct space using the software FOX [21] and treating BH₄ as a rigid body. After structure solution the respective models were refined with Fullprof [22] or TOPAS [23].

4. Conclusions

NH₄Ca(BH₄)₃ is to our knowledge the first perovskite-type inorganic compound that contains two inherently dynamic hydrogen-rich molecules, both on the anion and cation sites. The usage of ammonium NH₄⁺ as A-site cation allows stabilizing ammonium borohydride for the first time at room temperature and pressure. This describes an approach that is not restricted to perovskite-type borohydrides and the incorporation of NH₄⁺ may be generalized to search for new hydrogen-rich compounds. Besides the chemical benefit to hydrogen storage applications, the ammonium cation also

enriches the spectrum of structural tools by a further parameter, providing, next to the non-spherical borohydride anion, a cation with tetrahedral charge distribution. The combination of non-spherical ions with chemically distinct hydrogen species may be exploited in complex hydrides to design polar structures.

$\text{NH}_4\text{Ca}(\text{BH}_4)_3$ decomposes at 380 K to new ammonia-borane complex $\text{Ca}(\text{BH}_4)_2 \cdot \text{NH}_3\text{BH}_3$ and releases one hydrogen molecule in the process. A major drawback of boron and nitrogen-based hydrogen storage systems is the possible evolution of ammonia NH_3 and diborane B_2H_6 , which both lead to the failure of fuel cells. Neither of them are observed during the hydrogen release of $\text{NH}_4\text{Ca}(\text{BH}_4)_3$, while minor NH_3 evolution occurs during decomposition of $\text{Ca}(\text{BH}_4)_2 \cdot \text{NH}_3\text{BH}_3$, similar to previously reported AB-complexes of metal-borohydrides. $\text{NH}_4\text{Ca}(\text{BH}_4)_3$ is the first compound of a series of novel metal borohydrides which is expected to grow quickly thanks to a concept that is easily applied to a large and growing number of mixed-metal borohydride salts that contain cations similar in size and thus readily replaced by NH_4^+ . For instance, replacing NH_4^+ for K in $\text{K}_3\text{Mg}(\text{BH}_4)_5$ [24] or $\text{KAl}(\text{BH}_4)_4$ [25,26] would result in hydrogen densities of 21.2 and 19 wt %, which is already very close to NH_4BH_4 itself. Generally, the decomposition of such proposed compounds is assumed to be dominated by the transformation of NH_4^+ and BH_4^- to AB-complexes. While this mechanism is bound to release pure hydrogen, the subsequent decomposition of AB-complexes poses the known problems of rehydrogenation and fuel cell contamination.

Supplementary Materials

Supplementary materials can be accessed at: <http://www.mdpi.com/1996-1073/8/8/8286/s1>.

Acknowledgments

This work was supported by the Swiss National Science Foundation under project 200020_149218, by the Fonds National de la Recherche Scientifique (FNRS, Belgium) via instruments CC, PDR, EQP and by FRIA (Fonds pour la formation à la recherche dans l'Industrie et l'Agriculture, Belgium) funding FM's PhD works. The authors thank SNBL at the ESRF and SLS at the PSI for the beamtime allocation and Dmitry Chernyshov (SNBL), Vadim Dyadkin (SNBL) and Nicola Casati (SLS) for their assistance.

Author Contributions

P.S. and Y.S. performed the chloride based synthesis, F.M. performed the ammonium borohydride based synthesis. The synchrotron X-ray powder diffraction data were measured by P.S., Y.S., F.M., Y.F. and R.C. The diffraction data were analyzed by P.S. and R.C., crystal structures were solved by P.S. The manuscript has been written by P.S., and was commented by all authors.

Conflicts of Interest

The authors declare no conflict of interest.

References

1. Schlapbach, L.; Züttel, A. Hydrogen-storage materials for mobile applications. *Nature* **2001**, *414*, 353–358.
2. Schrauzer, G.N. Ueber ein periodensystem der metallboranate. *Naturwissenschaften* **1955**, *42*, 438.
3. Jepsen, L.H.; Ley, M.B.; Su-Lee, Y.; Cho, Y.W.; Dornheim, M.; Jensen, J.O.; Filinchuk, Y.; Jorgensen, J.E.; Besenbacher, F.; Jensen, T.R. Boron-nitrogen based hydrides and reactive composites for hydrogen storage. *Mater. Today* **2014**, *17*, 129–135.
4. Schouwink, P.; Ley, M.B.; Tissot, A.; Hagemann, H.; Jensen, T.R.; Smrčok, L.; Černý, R. Structure and properties of a new class of complex hydride perovskite materials. *Nat. Commun.* **2014**, *5*, 5706.
5. Dixon, D.A.; Gutowski, M. Thermodynamic Properties of Molecular Borane Amines and the $[\text{BH}_4^-][\text{NH}_4^+]$ Salt for Chemical Hydrogen Storage Systems from *ab Initio* Electronic Structure Theory. *J. Phys. Chem. A* **2005**, *109*, 5129–5139.
6. Karkamkar, A.; Kathmann, S.M.; Schenter, G.K.; Heldebrant, D.J.; Hess, N.; Gutowski, M.; Autrey, T. Thermodynamic and Structural Investigations of Ammonium Borohydride, a Solid with a Highest Content of Thermodynamically and Kinetically Accessible Hydrogen. *Chem. Mater.* **2009**, *21*, 4356–4358.
7. Flacau, R.; Ratcliffe, C.I.; Desgreniers, S.; Yao, Y.; Klug, D.D.; Pallister, P.; Moudrakowski, I.L.; Ripmeester, J.A. Structure and dynamics of ammonium borohydride. *Chem. Commun.* **2010**, *46*, 9164–9166.
8. Huang, Z.; Chen, X.; Yisgedu, T.; Meyers, E.A.; Shore, S.G.; Zhao, J.-C. Ammonium Octahydrotriborate ($\text{NH}_4\text{B}_3\text{H}_8$): New Synthesis, Structure, and Hydrolytic Hydrogen Release. *Inorg. Chem.* **2011**, *50*, 3738–3742.
9. Yisgedu, T.B.; Huang, Z.; Chen, X.; Lingam, H.K.; King, G.; Highley, A.; Maharrey, S.; Woodward, P.M.; Behrens, R.; Shore, S.G.; *et al.* The structural characterization of $(\text{NH}_4)_2\text{B}_{10}\text{H}_{10}$ and thermal decomposition studies of $(\text{NH}_4)_2\text{B}_{10}\text{H}_{10}$ and $(\text{NH}_4)_2\text{B}_{12}\text{H}_{12}$. *Int. J. Hydrog. Energy* **2012**, *37*, 4267–4273.
10. Nielsen, T.K.; Karkamkar, A.; Bowden, M.; Besenbacher, F.; Jensen, T.R.; Autrey, T. Methods to stabilize and destabilize ammonium borohydride. *Dalton Trans.* **2013**, *42*, 680–687.
11. Rude, L.H.; Nielsen, T.K.; Ravnsbæk, D.B.; Bösenberg, U.; Ley, M.B.; Richter, B.; Arnbjerg, L.M.; Dornheim, M.; Filinchuk, Y.; Besenbacher, F.; *et al.* Tailoring properties of borohydrides for hydrogen storage: A review. *Phys. Status Solidi* **2011**, *208*, 1754–1773.
12. Rude, L.H.; Filinchuk, Y.; Sørby, M.H.; Hauback, B.C.; Besenbacher, F.; Jensen, T.R. Anion Substitution in $\text{Ca}(\text{BH}_4)_2\text{-CaI}_2$: Synthesis, Structure and Stability of Three New Compounds. *J. Phys. Chem. C* **2011**, *115*, 7768–7777.
13. Xiong, Z.; Keong Yong, C.; Wu, G.; Chen, P.; Shaw, W.; Karkamkar, A.; Autrey, T.; Owen Jones, M.; Johnson, S.R.; Edwards, P.P.; *et al.* High-capacity hydrogen storage in lithium and sodium amidoboranes. *Nat. Mater.* **2007**, *7*, 138–141.
14. Wu, H.; Zhou, W.; Yildirim, H. Alkali and Alkaline-Earth Metal Amidoboranes: Structure, Crystal Chemistry, and Hydrogen Storage Properties. *J. Am. Chem. Soc.* **2008**, *130*, 14834–14839.

15. Wu, H.; Zhou, W.; Pinkerton, F.E.; Meyer, M.S.; Srinivas, G.; Yildirim, T.; Udovic, T.J.; Rush, J.J. A new family of metal borohydride ammonia borane complexes: Synthesis, structures, and hydrogen storage properties. *J. Mater. Chem.* **2010**, *20*, 6550–6556.
16. Grove, H.; Rude, L.H.; Jensen, T.R.; Corno, M.; Ugliengo, P.; Baricco, M.; Sørby, M.H.; Hauback, B.C. Halide substitution in $\text{Ca}(\text{BH}_4)_2$. *RSC Adv.* **2014**, *4*, 4736–4742.
17. Finlinchuk, Y.; Rönnebro, E.; Chandra, D. Crystal structures and phase transformations in $\text{Ca}(\text{BH}_4)_2$. *Acta Mater.* **2009**, *57*, 732–738.
18. Bowden, M.; Autrey, T. Characterization and mechanistic studies of the dehydrogenation of NH_xBH_x materials. *Curr. Opin. Solid State Mater. Sci.* **2011**, *15*, 73–79.
19. Schouwink, P.; Hagemann, H.; Embs, J.P.; D’Anna, V.; Černý, R. Di-hydrogen contact induced lattice instabilities and structural dynamics in complex hydride perovskites. *J. Phys. Condens. Matt.* **2015**, *27*, 265403.
20. Parry, R.W.; Schultz, D.R.; Girardot, P.R. The Preparation and Properties of Hexaminecobalt (III) Borohydride, Hexaminechromium (III) borohydride and Ammonium Borohydride. *J. Am. Chem. Soc.* **1958**, *1*, 1–3.
21. Favre-Nicolin, V.; Černý, R. FOX, “free objects for crystallography”: A modular approach to *ab initio* structure determination from powder diffraction. *J. Appl. Cryst.* **2002**, *35*, 734–743.
22. Rodriguez-Carvajal, J. *FULLPROF SUITE*; LLB Sacley & LCSIM: Rennes, France, 2003.
23. Coelho, A.A. TOPAS-Academic V5. 2012. Available online: <http://www.topas-academic.net/> (accessed on 15 February 2013).
24. Schouwink, P.; D’Anna, V.; Ley, M.B.; Lawson Daku, L.M.; Richter, B.; Jensen, T.R.; Hagemann, H.; Černý, R. Bimetallic Borohydrides in the System $\text{M}(\text{BH}_4)_2\text{-KBH}_4$ ($\text{M} = \text{Mg}, \text{Mn}$): On the Structural Diversity. *J. Phys. Chem. C* **2012**, *116*, 10829–10840.
25. Dovgaliuk, I.; Ban, V.; Sadikin, Y.; Černý, R.; Aranda, L.; Casati, N.; Devillers, M.; Filinchuk, Y. The first halide-free bimetallic aluminum borohydride: Synthesis, structure, stability, and decomposition pathway. *J. Phys. Chem. C* **2014**, *118*, 145–153.
26. Knight, D.A.; Zidan, R.; Lascola, R.; Mohtadi, R.; Ling, C.; Sivasubramanian, P.; Kaduk, J.A.; Hwang, S.-J.; Samanta, D.; Jena, P. Synthesis, Characterization, and Atomistic Modeling of Stabilized Highly Pyrophoric $\text{Al}(\text{BH}_4)_3$ via the Formation of the Hypersalt $\text{K}[\text{Al}(\text{BH}_4)_4]$. *J. Phys. Chem. C* **2013**, *117*, 19905–19915.